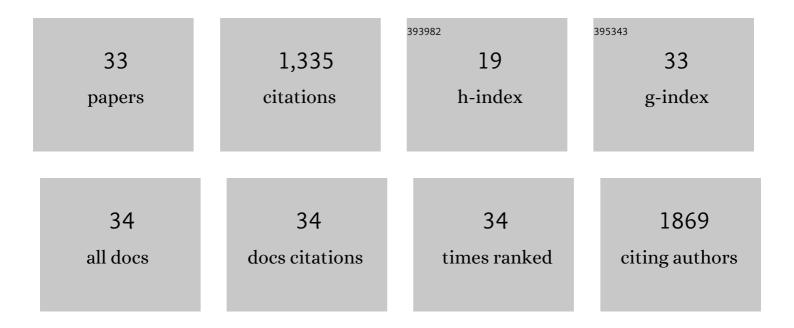
## De-Bo Hu

List of Publications by Year in descending order

Source: https://exaly.com/author-pdf/2122814/publications.pdf Version: 2024-02-01



DE-BO HU

#	Article	IF	CITATIONS
1	Far-field nanoscale infrared spectroscopy of vibrational fingerprints of molecules with graphene plasmons. Nature Communications, 2016, 7, 12334.	5.8	237
2	Modern Scatteringâ€Type Scanning Nearâ€Field Optical Microscopy for Advanced Material Research. Advanced Materials, 2019, 31, e1804774.	11.1	205
3	Ghost hyperbolic surface polaritons in bulk anisotropic crystals. Nature, 2021, 596, 362-366.	13.7	102
4	Broadly tunable graphene plasmons using an ion-gel top gate with low control voltage. Nanoscale, 2015, 7, 19493-19500.	2.8	90
5	Farâ€Field Spectroscopy and Nearâ€Field Optical Imaging of Coupled Plasmon–Phonon Polaritons in 2D van der Waals Heterostructures. Advanced Materials, 2016, 28, 2931-2938.	11.1	77
6	Probing optical anisotropy of nanometer-thin van der waals microcrystals by near-field imaging. Nature Communications, 2017, 8, 1471.	5.8	74
7	Simultaneous measurement of liquid level and surrounding refractive index using tilted fiber Bragg grating. Sensors and Actuators A: Physical, 2011, 170, 62-65.	2.0	53
8	Efficient Allâ€Optical Plasmonic Modulators with Atomically Thin Van Der Waals Heterostructures. Advanced Materials, 2020, 32, e1907105.	11.1	44
9	Flexible and Electrically Tunable Plasmons in Graphene–Mica Heterostructures. Advanced Science, 2018, 5, 1800175.	5.6	38
10	Study of graphene plasmons in graphene–MoS <sub>2</sub> heterostructures for optoelectronic integrated devices. Nanoscale, 2017, 9, 208-215.	2.8	36
11	Tunable Planar Focusing Based on Hyperbolic Phonon Polaritons in αâ€MoO <sub>3</sub> . Advanced Materials, 2022, 34, e2105590.	11.1	32
12	Active control of micrometer plasmon propagation in suspended graphene. Nature Communications, 2022, 13, 1465.	5.8	31
13	Tunable Modal Birefringence in a Low‣oss Van Der Waals Waveguide. Advanced Materials, 2019, 31, e1807788.	11.1	27
14	Hydraulic pressure sensor based on fiber Bragg grating. Optical Engineering, 2011, 50, 064401.	0.5	26
15	Ultrasensitive Poly(boric acid) Hydrogel-Coated Quartz Crystal Microbalance Sensor by Using UV Pressing-Assisted Polymerization for Saliva Glucose Monitoring. ACS Applied Materials & Interfaces, 2020, 12, 34190-34197.	4.0	26
16	High performance boronic acid-containing hydrogel for biocompatible continuous glucose monitoring. RSC Advances, 2017, 7, 41384-41390.	1.7	24
17	High-efficiency modulation of coupling between different polaritons in an in-plane graphene/hexagonal boron nitride heterostructure. Nanoscale, 2019, 11, 2703-2709.	2.8	24
18	Microdisplacement Sensor Based on Tilted Fiber Bragg Grating Transversal Load Effect. IEEE Sensors Journal, 2011, 11, 1776-1779.	2.4	23

De-Bo Hu

#	Article	IF	CITATIONS
19	Nanoimaging and Nanospectroscopy of Polaritons with Time Resolved <i>s</i> NOM. Advanced Optical Materials, 2020, 8, 1901042.	3.6	22
20	Ultrasensitive Midâ€Infrared Biosensing in Aqueous Solutions with Graphene Plasmons. Advanced Materials, 2022, 34, e2110525.	11.1	20
21	Refractive-Index-Enhanced Raman Spectroscopy and Absorptiometry of Ultrathin Film Overlaid on an Optical Waveguide. Journal of Physical Chemistry C, 2013, 117, 16175-16181.	1.5	19
22	30 s Response Time of K <sup>+</sup> lonâ€Selective Hydrogels Functionalized with 18â€Crownâ€6 Ether Based on QCM Sensor. Advanced Healthcare Materials, 2018, 7, 1700873.	3.9	15
23	Large cale Suspended Graphene Used as a Transparent Substrate for Infrared Spectroscopy. Small, 2017, 13, 1603812.	5.2	13
24	Probing Polaritons in 2D Materials. Advanced Optical Materials, 2020, 8, 1901416.	3.6	13
25	A Multibeam Interference Model for Analyzing Complex Nearâ€Field Images of Polaritons in 2D van der Waals Microstructures. Advanced Functional Materials, 2019, 29, 1904662.	7.8	10
26	The development of an antifouling interpenetrating polymer network hydrogel film for salivary glucose monitoring. Nanoscale, 2020, 12, 22787-22797.	2.8	10
27	Antifouling hydrogel film based on a sandwich array for salivary glucose monitoring. RSC Advances, 2021, 11, 27561-27569.	1.7	10
28	Low-fouling CNT-PEG-hydrogel coated quartz crystal microbalance sensor for saliva glucose detection. RSC Advances, 2021, 11, 22556-22564.	1.7	9
29	Hybrid hydrogel films with graphene oxide for continuous saliva-level monitoring. Journal of Materials Chemistry C, 2020, 8, 9655-9662.	2.7	8
30	Resonant Mirror Enhanced Raman Spectroscopy. Journal of Physical Chemistry C, 2014, 118, 13099-13106.	1.5	7
31	Structural colouration in the Himalayan monal, hydrophobicity and refractive index modulated sensing. Nanoscale, 2020, 12, 21409-21419.	2.8	6
32	Few-layer hexagonal boron nitride as a shield of brittle materials for cryogenic s-SNOM exploration of phonon polaritons. Applied Physics Letters, 2022, 120, .	1.5	2
33	Eigenmodes in a negative-refractive-index planar waveguide for high-sensitivity evanescent sensing and spectroscopic applications. Proceedings of SPIE, 2013, , .	0.8	1